ISSN (Online) 2456 -1304

International Journal of Science, Engineering and Management (IJSEM)
Vol 4, Issue 6, June 2019

Novel Method of Modelling For Wind and PV System

[1] John J Thanikkal, [2] Sruti VS, [3] Vidhun M
[1] IES College of Engineering, [2] IES college of Engineering, [3] IES college of Engineering
[1] johnjthanikal@yahoo.co.uk, [2] srutisubin@gmail.coml, [3]vidhunveru@gmail.com

***Abstract*—This paper presents a dynamic modelling and control strategy for a sustainable micro grid primarily powered by wind and solar energy. A current-source-interface multiple-input dc-dc converter is used to integrate the renewable energy sources to the main dc bus. Potential suitable applications range from a communication site or a residential area. A direct-driven permanent magnet synchronous wind generator is used with a variable speed control method whose strategy is to capture the maximum wind energy below the rated wind speed. This study considers both wind energy and solar irradiance changes in combination with load power variations. As a case study a 30-kW wind/solar hybrid power system dynamic model is explored. The examined dynamics shows that the proposed power system is a feasible option for a sustainable micro grid application.**

***Index Terms*—Photovoltaic power systems, power conversion, power system modelling, wind power generation**

1. INTRODUCTION

This paper presents a dynamic modelling and control strategy for a sustainable micro grid primarily powered by wind and photovoltaic (PV) energy. These sources are integrated into the main bus through a current-source-interface (CSI) multiple-input (MI) dc-dc converter. In order to provide the context for the discussion, the intended applications for this micro grid are a communication site or a residential area part of a future "smarter grid" [1]. The proposed micro grid is also equipped with energy storage devices, such as batteries. A utility grid connection is provided in order to replenish energy levels in case of power shortage from the renewable energy sources. Due to its diverse sources, power supply availability of such system may exceed that of the grid [2]. Outage possibility in this power system is close to zero because it is highly unlikely that all energy sources in this micro grid are unavailable at the same time. Moreover, the combination of wind generator and PV modules with local energy storage devices may reduce vulnerability to natural disasters [3], [4] because they do not require lifelines.

Among the earlier work in the literature, the idea of developing a sustainable micro grid for telecommunication applications using MI dc-dc converters was introduced in [4] and expanded in [5]. A variant of such system with a different MI converter (MIC) topology was later on described in [6] suggested a telecommunication power system in which a diesel generator and an automatic transfer switch were replaced with fuel cells and a micro-turbine using an MI dc-dc converter. The power systems in [4]–[6] had the following advantages: 1) the use of the MIC reduces unnecessary redundancy of additional parallel converters in each energy source, and 2) the investment in micro-sources is recuperated because the energy sources in this power system can be used during normal operation as well as grid power outages [3]–[6]. Nevertheless, one issue with such micro grid in [6] is that it still requires fuel for the local sources in normal operation.

In addition, the daily complementary generation profiles of a wind turbine and a PV module [7] have stimulated research on similar power systems with a dc link method rather than an ac coupling method [8]. However, these similar power systems in combined renewable energy sources with parallel single-input dc-dc converters which may lead to unnecessary redundancy in power system components. This problem can be resolved with an alternative combining method which uses MI dc-dc converters previously proposed in [2], [4]–[6], [7]– In addition, an MI dc-dc converter had other advantages such as the possibility of decentralized control and modularity. Despite these promising advantages, few studies [8] seem to have explored dynamic modelling techniques for a wind/solar hybrid power system with MI dc-dc converters-in contrast to those with parallel converters. Although the hybrid power systems in [6] and [7] considered a wind generator as a local source for an MIC, they did not consider wind energy variations and ac system characteristics such as ac wind generators, local ac load power variations, and interaction with the distribution grid, which likely affect the controllability and performance of the micro grid

This paper presents a dynamic modelling and operation strategy of a wind/solar hybrid power system with an MI dc-dc converter in which wind energy changes, ac wind generator, and variations in the local ac load power and dispatch power to the distribution grid are considered. A

ISSN (Online) 2456 -1304

International Journal of Science, Engineering and Management (IJSEM)
Vol 3, Issue 6, June 2019

direct-driven permanent magnet synchronous generator (PMSG) is used for the wind generator model because a direct-driven PMSG has drawn attention for the residential-scale power level due to its gearless system. In addition of wind energy variations, this study also considers the rapid changing solar irradiance that may happen during the day and that affects generated power from PV modules in the proposed power system. Moreover, the herein proposed micro grid does not require any fuel for the local sources because it is powered by inherently self sustainable energy sources. Thus, with enough local energy storage, it does not rely on lifelines—e.g., roads or pipes for fuel or natural gas delivery for operation, which makes it a truly self sustainable power system ideal to provide power not only in normal conditions but also during extreme events when lifeline operation is poor or not expected.

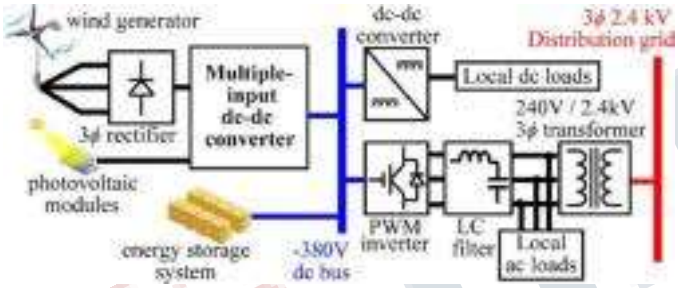

Fig. 1. Overall architecture of the proposed sustainable micro grid

Furthermore, the proposed power system not only can produce electricity from the renewable energy sources but may also inject surplus power to the utility grid in normal operation.

The rest of this paper is organized as follows. The overall architecture of the proposed sustainable micro grid and the modelling components of this system are discussed in Section and III respectively. The control strategies of the proposed micro grid are discussed in Section IV, and simulation results and discussions about the proposed micro grid are included in Section V in order to illustrate the dynamics of the proposed sustainable power system. A case study of a 30-kW wind/solar hybrid micro grid model is developed and explored in Section V. Section VI concludes with the summary of findings.

2. PROPOSED SUSTAINABLE MICRO GRID ARCHITECTURE

Fig. 1 shows the overall architecture of the proposed micro grid with wind and PV resources. Its main energy sources, wind and solar radiation, are transformed in a wind generator and PV modules. In order to combine these energy sources, a CSI MIC, such as an MI Ćuk converter or an MI SEPIC converter [15] with a dc bus system, is used because a CSI MIC is more effective for maximum power point (MPP) tracking in PV modules and for the input current control method used in this micro grid. MICs were chosen because they provide a cost-effective and flexible method to interface various renewable energy sources [4], [5], [8]. In addition, a dc power distribution system is chosen because dc power systems may achieve higher availability and energy efficiency in a simpler way than equivalent ac power systems [2].

A voltage level of 380 V is considered to be the main dc bus voltage in this power system because it is more suitable for bidirectional power flow between the intended power system and the utility grid [5] and because it is the likely voltage to be chosen in a future standard for industrial applications with dc distribution, such as in data centres. However, a three-phase rectifier in the wind generator may be required for this dc distribution system because the output voltage of the wind generator is usually ac. As depicted in Fig. 1, an energy storage system (ESS) is also connected to the main dc bus in order to overcome the intermittent properties of renewable energy sources and to support local power production in an islanded mode particularly during blackouts or natural disasters. Depending on applications, the various voltage levels of local dc loads such as 48 V telecommunication power systems or plug-in electric vehicles can be accommodated through an additional dc-dc converter as described in Fig. 1.

The local ac loads whose line-to-line voltage level is in this micro grid can also be connected with a PWM inverter and an LC filter used to reduce harmonic voltages produced at the local ac bus. As shown in Fig. 1, this local ac distribution system may also be tied to the three-phase 2.4 kV distribution grid with a three-phase 240 V/2.4 kV transformer that also contributes to filter harmonic content in the inverter output and to reduce filter needs in the LC filter.

3. MODELLING COMPONENTS OF THE PROPOSED MICRO GRID

This section reviews major modelling components which are used in Section V in order to realize its system-wide micro grid model.

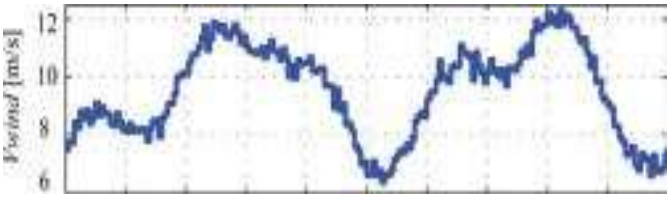

Fig. 2. Wind model used for the simulation study

ISSN (Online) 2456 -1304

International Journal of Science, Engineering and Management (IJSEM)
Vol 3, Issue 6, June 2019

A. Wind Model

This paper uses a wind model presented in [2] in order to simulate the spatial effect of wind energy variations such as gusting, rapid ramp changes, and background noises. This wind model is defined by (1) where is a constant wind velocity, is a gust wind component which can be implemented by a cosine function, is a ramp wind component used for mimicking rapid wind changes, and is background noises of wind. Fig. 2 shows this wind model used for the simulation study which will be discussed in Section V.

$$V_{\text{wind}} = V_{\text{base}} + V_{\text{gust}} + V_{\text{ramp}} + V_{\text{noise}} \quad (1)$$

B. Wind Turbine Model

A wind turbine in the proposed micro grid simulation study is modelled by an aerodynamic input torque which drives a wind generator. In order to explain the wind turbine model here, the mechanical power captured by the blades of a wind turbine is described as follows [1]: (2) where is a rotor power coefficient, is a blade pitch angle, is a tip-speed ratio (TSR), is an air density, is the radius of a wind turbine blade, and is a wind speed. The rotor power coefficient is defined by the fraction of the available wind power that can be transformed to the mechanical power by a rotor [2]. This rotor power coefficient depends on the blade aerodynamics, which is the function of a blade pitch angle and a TSR [9], [2]. The type of a wind turbine rotor may also be another factor affecting the rotor power coefficient. However, the of [2] in which a general blade type was assumed is used in this study for the sake of simplicity [6]

$$P_m = \frac{1}{2} C_p(\beta, \lambda) \rho \pi R^2 V_{\text{wind}}^3 \quad (2)$$

$$C_p = (0.44 - 0.0167\beta) \sin \frac{\pi(\lambda - 2)}{13 - 0.3\beta} - 0.00184(\lambda - 2)\beta. \quad (3)$$

$$\lambda = \frac{\omega_m R}{V_{\text{wind}}} \quad (4)$$

$$T_m = \frac{C_p(\beta, \lambda) \rho \pi R^5}{2\lambda^3} \omega_m^2. \quad (5)$$

TABLE I .PARAMETERS AND SPECIFICATIONS OF THE WIND TURBINE MODEL

parameter name	value	unit
rated power	20	kW
rated wind speed	12	m/s
rated rotor speed	27.5413	rad/s
blade radius	3.7	m
blade pitch angle	0	degree
air density	1.225	kg/m^3

parameter name	value	unit
rated power	20	kW
rated line voltage	519.6	V_{rms}
stator phase inductance	8.5	mH
stator phase resistance	0.35	Ω
number of poles	12	
rated mechanical speed	263	rpm
electrical base frequency	26.3	Hz

The TSR can be defined as the function of a wind speed [9], written as (4) where is the rotor speed of a wind turbine. Then, from (2), (4), and considering that , the aerodynamic input torque by which a wind generator is driven can be obtained as follows [9]: (5) The wind turbine in the simulation study is modelled by (5) in which the input variables are the wind turbine rotor speed and the TSR that can be calculated with (4). The parameters of the investigated wind turbine model in this paper are shown in Table I. According to (3) and, the aerodynamic torque is maximized at a given wind speed when the pitch angle of a blade is 0 . Therefore, a constant pitch angle is used in this study as shown in Table I.

C. Direct-Driven PMSG

The wind generator considered here is a gearless direct-driven PSMG. This PMSG does not require frequent mechanical maintenance because it does not use gears between wind blades and the generator. Another advantage of the direct-driven PMSG is that a permanent magnet eliminates the dc excitation circuit that may complicate the control hardware [3]. Table II shows the specifications of the direct-driven PMSG model used in the simulation study. For the simulation study, the internal model of a PMSG in MATLAB Simulink/Simpower systems is used with the specifications provided in Table II.

D. PV System Model

This study uses the PV model that is depicted in Fig. 3 and was proposed in [4] because it is suitable for simulating

ISSN (Online) 2456 -1304

International Journal of Science, Engineering and Management (IJSEM)
Vol 3, Issue 6, June 2019

practical PV systems which are composed of numerous PV modules and because it only requires a few parameters, such as the number of PV modules, PV array open-circuit voltage and short-circuit current [4]. Moreover, this model can represent solar irradiance and temperature changes which may happen commonly during the day [24]. The detailed discussions of this PV model are out of the scope of this paper; however, a reader may refer to [4] for explanation of such model derivations. The rated power of the PV system in this paper is 10 kW, which is composed of 50 KC200GT modules manufactured by Kyocera Solar Energy Inc. The simulated PV system configuration is an array of 5 10 modules, and its voltage and current at the MPP with the solar irradiance of are 261.3 V and 38.1 A, respectively.

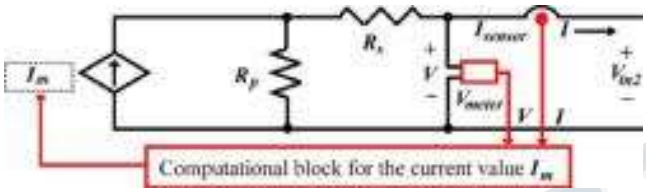

Fig. 3. Circuit-based PV model [24] used in the simulation study.

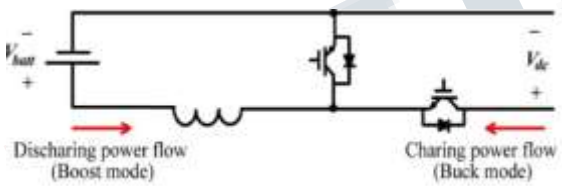

Fig 4. ESS Model

E. ESS Model

This study considers batteries as energy storage devices. However, these batteries may require a dc-dc power converter in order to step up their voltage to the main dc bus voltage because their nominal voltage whose level is 240V in this micro grid is typically lower than the main dc bus voltage. One reason for using a lower battery voltage is to improve their reliability and life-time by avoiding issues found in higher voltage configurations, such as cell voltage equalization. For this purpose, a bidirectional boost/buck converter shown in Fig. 4 is considered in the proposed micro grid. If the power generation from the renewable micro-energy sources is insufficient for the demand power at the load side, this bidirectional converter operates in a boost mode in order to discharge energy from batteries to the main dc bus as depicted in Fig. 4.When the renewable power production exceeds the load-side demand power, this power converter works in a buck mode in which power flows from the main dc bus to charge the batteries with the extra local power production.

F. MI CSI Converter

Among MIC topologies in [2], [4]–[6], and [12]–[19], MI CSI converters such as an MI Ćuk converter [2], [5] and an MI SEPIC converter [5], [1] can be used in this micro grid. These MI CSI converters provide nearly continuous input current waveforms due to their CSI input legs. Hence, these converters provide more operational flexibility than an MI buck-boost converter [3] because they allow the integration of input sources that require a relatively constant current [2], such as the input current control that is used in this power plant and is explained in Section IV-A. An MI Ćuk Converter is similar to an MI SEPIC converter [1], [8] except for the output voltage inversion.

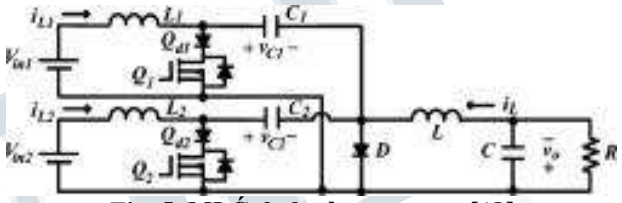

Fig. 5. MI Ćuk dc-dc converter [12]

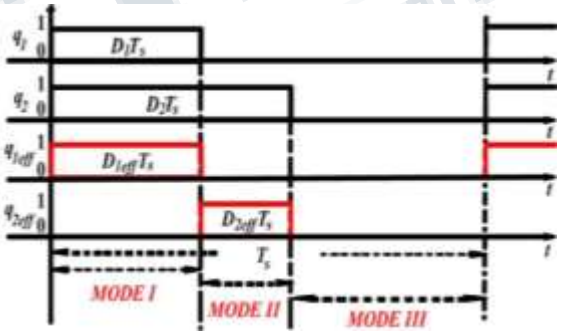

Fig. 6. Switching diagram of the MI Ćuk dc-dc converter

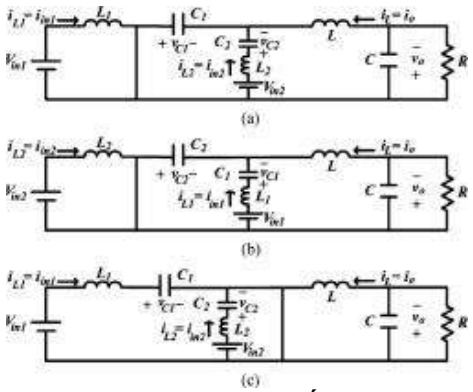

Fig. 7. Operational modes of MI Ćuk dc-dc converter. (a) Mode I (only conducts current). (b) Mode II (only conducts current) (c) Mode III (only diode conducts current).

ISSN (Online) 2456 -1304

International Journal of Science, Engineering and Management (IJSEM)
Vol 3, Issue 6, June 2019

However, since there are more past works focusing exclusively on the MI SEPIC [8], the analysis here focuses on the MI Ćuk converter shown in Fig. 5. Fig. 6 illustrates the switching diagram of an MI Ćuk converter. If it is assumed to be operated in a continuous conduction mode, circuit operation in a steady state can be described based on the following three operational modes.

Mode 1 (see Fig. 7(a);): It is assumed that the voltage level of the first input source is higher than that of the second input source .Although active switches and are turned on in this mode as depicted in Fig. 6, only conducts current since the diode is reverse-biased due to the assumption that is greater than. The diode at the common output stage is also reverse-biased.

Mode 2 (see Fig. 7(b);): As illustrated in Fig. 6, only an active switch is turned on and conducts current in this mode since the diode is also turned on. The diode at the common output stage is still reverse-biased.

Mode 3 (see Fig. 7(c) ;): All switches except the diode are turned off in this mode. Therefore, the diode only conducts current. Based on the described operational modes, the switched dynamic model of this MI Ćuk converter is governed by where and are the switching functions of the MI Ćuk converter, and are the effective switching functions of each input cell that equal and respectively. In an average sense, the derivatives of an inductor current and a capacitor voltage are zero. In addition, switching functions and can be considered as duty cycles and respectively in the average model.

4. CONTROL STRATEGIES

A. Wind Turbine: Variable Speed Control

This paper uses a variable speed control method whose strategy is to capture the maximum wind energy below the rated wind speed. Fig. 8 shows mechanical power captured by wind turbine blades at each rotor speed of the wind turbine and various wind speeds. As Fig. 8 illustrates, mechanical power from the wind turbine depends on the wind turbine rotor speed. In addition, the optimal power line can be obtained by connecting MPPs at each wind speed because a single MPP exists at each wind speed as shown in Fig. 8. Hence, the operation of the wind turbine at the optimal rotor speed on the optimal power curve ensures that the wind turbine captures the maximum wind energy below the rated wind speed. One feasible method to operate the wind turbine on the optimal power line below the rated wind speed is to control the three-phase rectified output current with the wind turbine rotor speed [9], [2]. In order to describe such control method, the optimal mechanical power of the wind turbine is considered to be [5] where the maximum rotor power coefficient, is the optimal TSR, is an optimal power constant, is air density, and is the radius of a wind turbine blade.

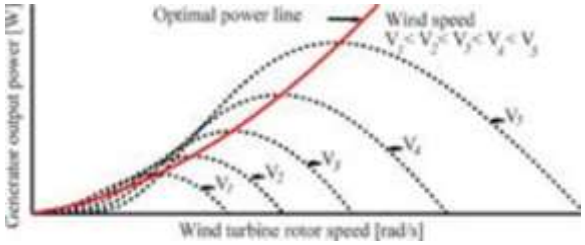

Fig. 8. Mechanical power of a wind turbine at various wind speeds [2].

If power efficiencies of the wind generator and the three-phase rectifier in Fig. 1 are assumed to be constant at and respectively, the optimal real power at the three-phase rectifier output, where and are the rectified output voltage and current respectively. If a PMSG is assumed to be an ideal generator, the line-to-line voltage and where is the voltage constant of the generator, is the electrical angular frequency of the generator, and is the number of poles in the generator. Then, the three-phase rectified output voltage where is the peak line-to-line voltage, and is the stator phase inductance of the PMSG. By solving the quadratic equation that can be obtained from (2) and (4) with respect to, the reference rectified current results to be equal to

$$I_{R_{opt}} = \frac{3pK_v - \sqrt{(3pK_v)^2 - 24p\pi\eta_G\eta_R K_{opt} L_s \omega_m^2}}{6pL_s}$$

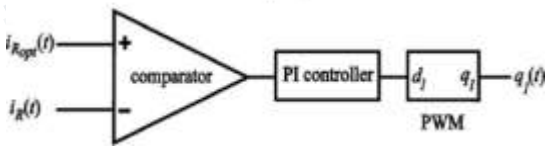

Fig. 9. Current mode controller

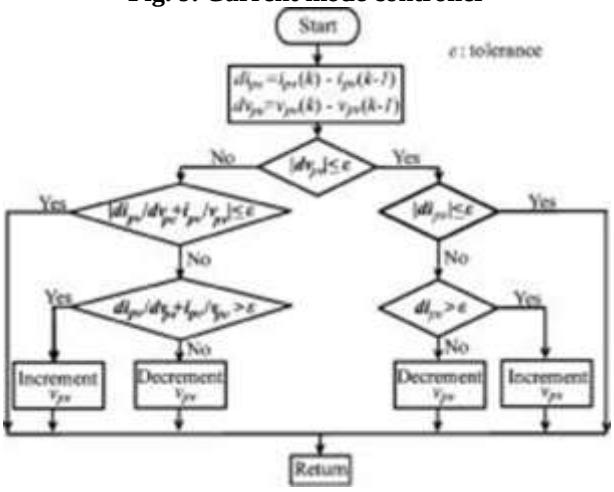

Fig. 10. Flow chart of an incremental conductance method

ISSN (Online) 2456 -1304

International Journal of Science, Engineering and Management (IJSEM)
Vol 3, Issue 6, June 2019

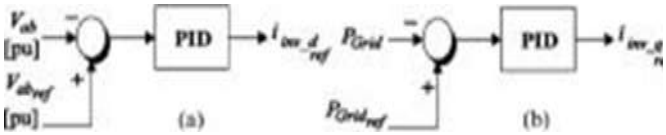

Fig. 11. - Inverter current controller. (a) Voltage controller. (b) Active power controller

Hence, the wind turbine can be operated along the optimal power curve if is controlled to its reference value by adjusting the duty ratio of the MIC at each according to the equation. This paper uses a PI controller, shown in Fig. 9, in order to achieve this target current. Hence, the wind turbine can be operated along the optimal power curve if is controlled to its reference value by adjusting the duty ratio of the MIC. This paper uses a PI controller, shown in Fig. 9, in order to achieve this target current.

B. PV Module: MPP Tracking

The PV system is also controlled so that it operates at its MPP. An incremental conductance method is selected for this purpose. It uses the PV modules output current and voltage information based on polarity changes in the derivative of power with respect to their voltage, which is zero at the MPP, positive at the left of the MPP, and negative at the right of the MPP. These voltage polarity changes characteristics lead to the following criterion that identifies whether PV panels reach their MPP or not.

Once the MPP is calculated with this method, the MIC controller regulates PV modules' output voltage towards the obtained reference voltage by adjusting the MIC's duty ratios. The detailed flow chart of this control method is provided in Fig. 10. As indicated in Fig. 10, a tolerance which equals zero is used for this criterion in the simulation study because this tolerance allows PV modules to remain at their MPP once they reach their MPP. Otherwise, PV modules may oscillate around their MPP when they reach their MPP, thus producing steady-state error at the operating points of the PV system. Practical ways of addressing this issue in real situations [8] have extensively been studied in the past and are out of the scope of this paper.

C. ESS Control

The ESS in this micro grid is controlled to regulate the main dc bus voltage both when there is not sufficient power production from the wind generator and PV modules and when there is excess local power production to charge the batteries. A bidirectional boost/buck converter shown in Fig. 4 is used with the hysteresis control in [9]. If is higher than an upper voltage limit, ESS will be charged in a buck mode so that is regulated toward. If is lower than a lower voltage limit, ESS will be discharged in a boost mode in order to regulate toward. Otherwise, ESS will be in a float mode.

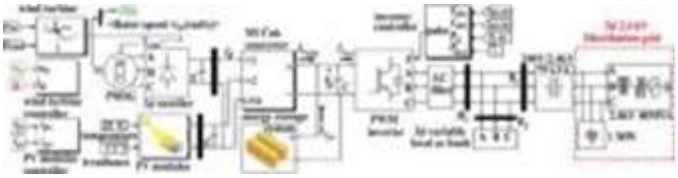

Fig. 12. Configuration of the simulated 30-kW sustainable micro grid

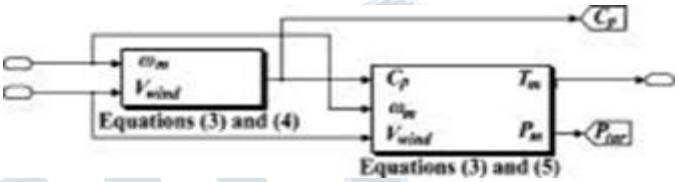

Fig. 13. Block diagram of the wind turbine in Fig. 12

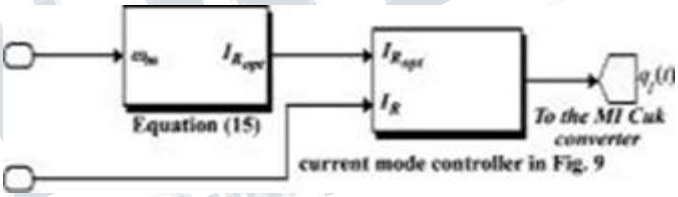

Fig. 14. Block diagram of the wind turbine controller in Fig. 12

D. PWM Inverter Control

The primary goal of a PWM inverter controller is to regulate three-phase local ac bus voltage and frequency in this micro grid and to dispatch target active power to the distribution grid, which may be set by users or grid operators. For these purposes, based current control is used in the PWM inverter.

As described in Fig. 11(a), a local ac line-to-line voltage is regulated by the component of the reference inverter current in the frame. Dispatch active power to the grid can also be controlled by the component of the reference inverter current as depicted in Fig. 11(b).

5. RESULTS AND DISCUSSIONS

Fig. 12 shows the overall configuration of the simulated 30-kW wind/solar power system. In order to focus on local ac load and grid injected power variations, this study did not consider local dc loads in the simulation because dc loads can be trivially connected to the main dc bus if its dc voltage is regulated. The wind turbine is modelled by (3), (4), and (5) as indicated in Fig. 13. Detailed specifications of the wind

ISSN (Online) 2456 -1304

International Journal of Science, Engineering and Management (IJSEM)
Vol 3, Issue 6, June 2019

turbine and the PMSG are shown in Tables I and II, respectively. Fig. 14 depicts the wind turbine controller developed based on (15) and the current mode controller shown in Fig. 9. Fig. 15 illustrates the digital PV module controller that is realized based on the incremental conductance control in order to track the MPPs of solar energy as discussed in Section VI-B. The MI Ćuk converter is modelled with built-in circuit-based components in MATLAB Simulink/Simpower systems, and the circuit schematic and component values are illustrated in Fig. 16. The internal models of a PMSG, a three-phase rectifier, a PWM inverter, and a three-phase 240V/2.4 kV transformer in MATLAB Simulink/Simpower systems are used for this study. The circuit-based PV model shown in Fig. 3 is used for this study with the parameters presented in the previous Section III-D.

Therefore, the output power from the wind turbine increases when the wind speed also increases. Similarly, when wind speed decreases, the reference input current declines, thus decreasing the rectified output current and the terminal rectified output voltage. Hence, the output power from the wind turbine declines when wind speed decreases. Therefore, it can be concluded that the wind generator operates in the optimal power point despite different environmental conditions such as sudden increases or decreases of the wind speed, which likely happen during the day. Moreover, the wind generator controller expeditiously reacts to such rapid changing environmental conditions.

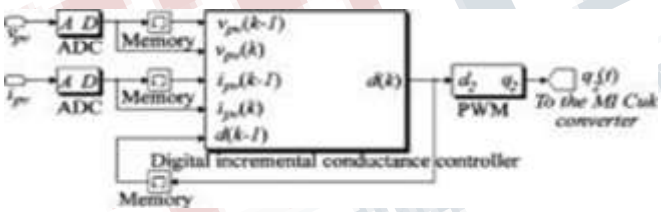

Fig. 15. Block diagram of the PV panel controller in Fig. 12. ADC Analog-todigital converter. PWM: Pulse width modulator

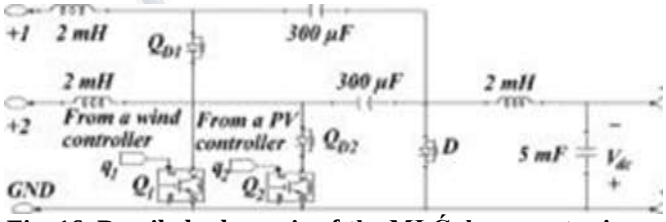

Fig. 16. Detailed schematic of the MI Ćuk converter in Fig. 12

A. Control Performance of the Wind Turbine

A wind model presented in Section III.A is considered to simulate the spatial effect of varying wind components. As indicated in Fig. 17(a), (b), and (f), when wind speed increases, the wind turbine rotor speed accelerates so that the output power from the wind turbine increases. On the other hand, when wind speed decreases, the wind turbine rotor speed slows down so the output power from the wind turbine decreases. The wind turbine is also operated at the optimal rotor speed and harvests the maximum power from wind energy at each wind speed since a rotor power coefficient keeps constant at 0.44, which is its maximum possible value as shown in Fig. 17(c).

Fig. 17 also shows the output terminal electrical characteristics of the three-phase rectifier with wind energy variations. As shown in Fig. 17(a) and (d), the reference input current elevates when wind speed increases. Thus, the rectified output current is controlled toward the reference current, and the terminal rectified output voltage increases as indicated in Fig. 17(e).

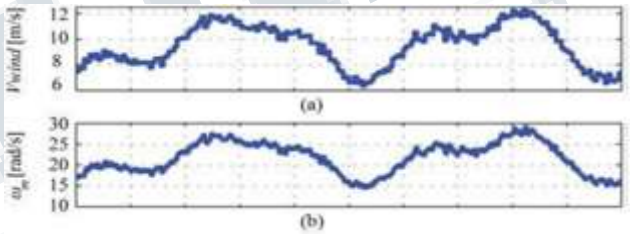

Fig. 17. Wind turbine control performance (a) Wind speed. (b) Turbine rotor speed. (c) Wind turbine rotor power coefficient. (d) Reference current and three-phase rectified output current. (e) Three phase rectified output voltage. (f) Wind turbine power

B. Control Performance of the PV Modules

This study also investigates the system performance with solar irradiance variations. The PV panel surface temperature is assumed to be fixed at during the entire simulation period. Fig. 18 shows the control performance of PV modules with solar irradiance variations whose data sets [2] were collected at Golden, CO, by NREL from 12:41 pm to 1 pm MST on July 31, 2008. The PV modules operating power points are well-followed toward the MPPs because described in (16) is almost zero even when the solar irradian

ISSN (Online) 2456 -1304

International Journal of Science, Engineering and Management (IJSEM)
Vol 3, Issue 6, June 2019

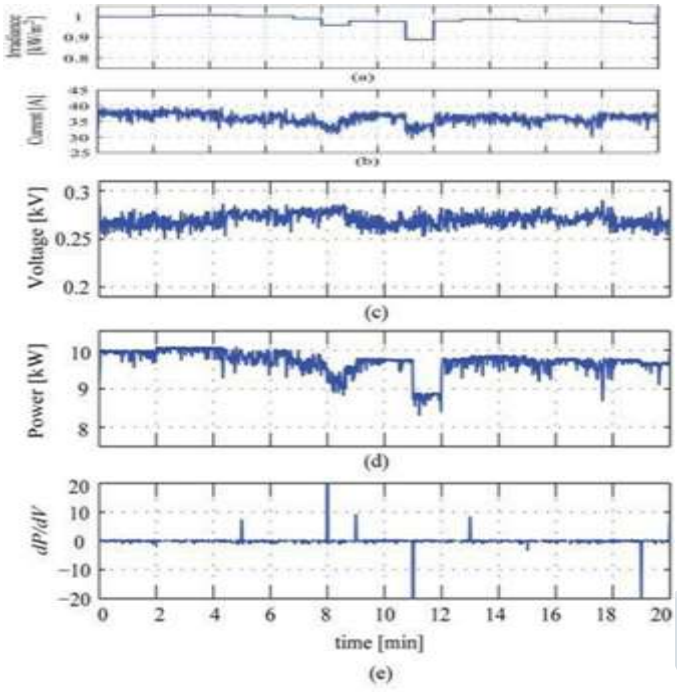

Fig. 18. PV modules control performance (a) Solar irradiance. (b) PV modules current. (c) PV modules voltage. (d) PV modules power. (e)

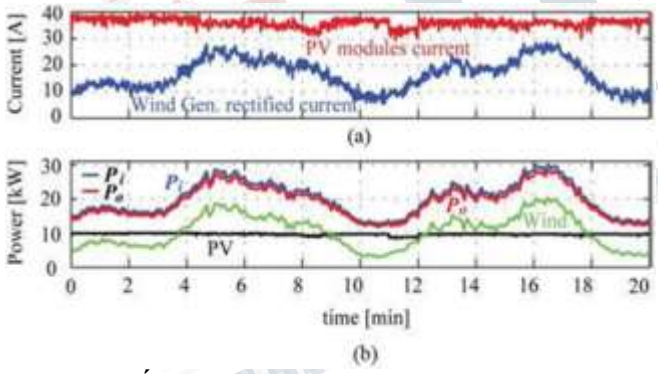

Fig. 19. MI Ćuk converter (MIC) control performance (a) MIC input currents: PV modules current and wind generator rectified current.

MIC input and output power, wind turbine power, PV modules power changes as attested in Fig. 18(a) and (e). Thus, this PV system controller tracks the MPPs of solar energy regardless of the rapidly changing wind energy. Specifically, this PV system controller immediately locates the MPP since this PV system is independently controlled. Considering that the performances of these wind and PV controllers illustrated in Figs. 17 and 18, it is verified that the discussed control strategy is an adequate one for a wind/solar micro grid with a CSI MIC.

C. Control Performance of the MI Ćuk Converter

Fig. 19 shows the control performance of the MI Ćuk converter when wind speed and solar irradiance change in the same manner than in Figs. 17 and 18. Fig. 19(b) shows the input and output power of the MI Ćuk converter, the wind turbine power, and the PV modules' power. There seem to be differences between and due to the switching and conduction losses in active circuit components, as shown in Fig. 16.

6. CONCLUSION

This paper presented the dynamic modelling and operational strategy of a sustainable micro grid primarily powered by wind and solar energy. These renewable sources are integrated into the main dc bus through an MI CSI dc-dc converter. Wind energy variations and rapidly changing solar irradiance were considered in order to explore the effect of such environmental variations to the intended micro grid. In addition, the proposed micro grid is equipped with an ESS and is connected with the distribution grid. These diverse micro-energy resources can improve the micro grid performance and reduce power generation variability and vulnerability to natural disasters. Its power converter can also be designed in a smaller size with low production costs because MICs can remove unnecessary redundant components. A 30-kW wind/solar hybrid micro grid dynamic model was developed with MATLAB Simulink/Simpower systems. For this purpose, this paper focused on the MPP tracking of the renewable micro-energy source power variations under the local ac demand changes and the variable dispatch power to the distribution grid. For the wind generator, this paper used a variable speed control method whose strategy is to capture the maximum wind energy below the rated wind speed. Specifically, an input current control method was used for this variable speed control. In addition, a circuit-based PV system model with an incremental conductance control method was used for the simulation study. In contrast to previous works, this paper explored the system wide performance of the sustainable micro grid with an MI dc-dc converter when the micro-energy source power, the local ac load, and the dispatch power to the distribution grid change. In addition, this study also considered an ac wind generator and a grid-side inverter in the proposed model. The system-wide simulated dynamics in Section V attested that the control strategy proposed in this paper is feasible when deploying a sustainable micro grid with a CSI MI dc-dc converter which can reduce its production costs.

REFERENCES

1. A. Kwasinski, "Identification of feasible topologies for multipl-input DC-DC converters," IEEE Trans. Power Electron., vol. 24, no. 3, pp. 856–861, Mar. 2009.

2. A. Kwasinski and P. T. Krein, "A micro grid-based telecom power system using modular multiple-input DC-DC converters," in Proc. IEEE 27th INTELEC, 2005, pp. 515–520

3. C. Yaow-Ming, L. Yuan-Chuan, H. Shih-Chieh, and C. Chung-Sheng, "Multi-input inverter for grid-connected hybrid PV/Wind power system," IEEE Trans. Power Electron., vol. 22, no. 3, pp. 1070–1077, May 2007.

4. C. Liu, K. T. Chau, and Z. Xiaodong, "An efficient wind-photovoltaic hybrid generation system using doubly excited permanent-magnet brushless machine," IEEE Trans. Ind. Electron., vol. 57, no. 3, pp. 831–839, Mar. 2010.

5. S.-K. Kim, J.-H. Jeon, C.-H. Cho, J.-B. Ahn, and S.-H.

6. Kwon, "Dynamic modelling and control of a grid-connected hybrid generation system with versatile power transfer," IEEE Trans. Ind. Electron., vol. 55, no. 4, pp. 1677–1688, Apr. 2008.

7. E. Muljadi and J. T. Bialasiewicz, "Hybrid power system with a controlled energy storage," in Proc. IEEE 29th IECON, 2003, vol. 2, pp. 1296–1301.

8. C. Yaow-Ming, L. Yuan-Chuan, H. Shih-Chieh, and C. Chung-Sheng, "Multi-input inverter for grid-connected hybrid PV/Wind power system," IEEE Trans. Power Electron., vol. 22, no. 3, pp. 1070–1077, May 2007.

9. M. E. Haque, M. Negnevitsky, and K. M. Muttaqi, "A novel control strategy for a variable-speed wind turbine with a permanent-magnet synchronous generator," IEEE Trans. Ind. Appl., vol. 46, no. 1, pp. 331–339, Jan./Feb. 2010.

10. B. G. Dobbs and P. L. Chapman, "A multiple-input DC-

11. DC converter topology," IEEE Power Electron. Lett., vol. 1, no. 1, pp. 6–9, Mar. 2003.

12. F. Valenciaga and P. F. Puleston, "Supervisor control for a stand-alone hybrid generation system using wind and photovoltaic energy," IEEE Trans. Energy Convers., vol. 20, no. 2, pp. 398–405, Jun. 2005.